IAC-16-B3.7.11

SOFT AND MINIMUM REACTIONS ROBOTIC CAPTURE OF NON-COOPERATIVE SPACECRAFTS

Silvio Cocuzza
University of Strathclyde, United Kingdom
silvio.cocuzza@strath.ac.uk

Mutian Li
University of Strathclyde, United Kingdom
mutian.li@strath.ac.uk

Xiu-Tian Yan
University of Strathclyde, United Kingdom
x.yan@strath.ac.uk

ABSTRACT

The capture of non-cooperative targets is a key priority for future space robotics missions. Typical operative scenarios are the maintenance and refuelling of malfunctioning satellites or the capture of space debris. In these operative scenarios, one of the key issues to be addressed is the impact force minimization: a null relative velocity of the robot end-effector with respect to the target is required at the time of capture, otherwise either the target or the robotic system could be damaged, the target could be pushed away, or the chaser spacecraft attitude could be destabilized. On the other hand, it is always desirable that the reaction torques transferred by the manipulator to the base spacecraft are minimized, so that a small amount of fuel is used for the attitude recovery, which is required to maintain the communication link with the ground after the robotic manoeuvre, thus increasing the system operating life. In this paper, two novel methods are proposed and compared for capturing a non-cooperative target with a redundant robot and in the meantime transferring a null reaction torque to the base spacecraft. This is a great advantage with respect to the state of the art capture methods, in which the problem of capture and of reactions minimization are handled separately and their integration is not straightforward. In the first method, the robot end-effector follows a parametric trajectory, which parameters are computed in order to have the same direction and speed of the target at the time of capture. On the other hand, in the second method the end-effector trajectory is computed by making the position and velocity error converge to zero inside the inverse kinematics control loop. The proposed methods have been demonstrated and compared by means of dynamic simulations of a 3-degrees-of-freedom planar manipulator. Both of them have shown a good performance and in particular in both cases the manipulator is able to reach the target with the desired end-effector velocity and with a null reaction torque transferred to the base spacecraft.

INTRODUCTION

Transferring minimum reactions to the spacecraft during a manipulator manoeuvre is an important issue in order to maintain the antennas communication link, keep the orientation of pointing instrumentation, scanning devices, and solar panels. Reduced reactions result in reduced energy consumption and longer operating life of the Attitude Control System (ACS) [1-3]. Several solutions to the redundant Inverse Kinematics (IK) problem have been proposed in literature according to a kinematic approach, for the local minimization of the spacecraft attitude

disturbance exploiting the momentum and angular momentum conservation laws [4-8], and according to a dynamic approach [9-24], whose aim is to minimize the reaction forces and torques transferred to the base spacecraft.

In the operating scenario of a target approach manoeuvre, the *free-floating mode*, i.e. manipulation with the ACS and the propulsion system turned off, is more adequate than the *free-flying mode* (ACS and propulsion system on) in the final approach phase both because it leads to more accurate end-effector positioning [3] and for safety reasons. Moreover, undesirable robot and ACS controller interaction may arise when they work simultaneously [25].

Recently one of the authors proposed an original Least Squares (LS) based IK solution for the local minimization of the reactions transferred to the base spacecraft by redundant manipulators [15]. This solution, which is applicable with generality to any 3D free-floating robot, has been experimentally validated for a 2D fixed-based robot. The robot used for the validation, which has three Degrees of Freedom (DOF) and one degree of redundancy, has been suspended by means of air bearings in order to perform simulated microgravity tests and fixed to ground by means of a dynamometer for the measure of the forces and torques tranferred to ground [26-28].

Two characteristics make the proposed IK solution very appealing. The first is that the solution can be extended in order to take into account the robot physical/mechanical constraints in the form of joint angle, velocity, and acceleration limits directly inside the solution algorithm [15,29,30], and this may be also useful for avoiding algorithmic instabilities [31,32]. The second one is that the presented solution, and its extension which takes into account the joint limits, results to be suitable for real-time implementation by means of recursive algorithms [33], by means of solution techniques used for the more general constrained Quadratic Programming problem [34-38], or by means of neural networks algorithms [29,39-41].

The analysis of the proposed IK solution in the case of multi-DOF manipulators has been presented in [42-47]. In particular, a preliminary study of the main operational parameters that can be used to maximize the Zero Reaction Workspace (ZRW) [23] of a multi-DOF 3D space manipulator has been presented in [47]. In [48] a novel method has been presented for the capture of a non-collaborative spacecraft with a redundant space manipulator using (i) a reactionless motion of the manipulator (based on the proposed IK solution), (ii) an optimal control of the end-effector path, and (iii) Kalman filtering techniques in order to reduce the measurement error on the position and velocity of the target satellite. Moreover, some strategies to increase the robustness of the proposed IK solution have been presented in [49-51].

The optimization algorithms used for the development of the proposed IK solution in the case of space robots can be also applied to the minimization of contact forces of climbing robots [52] and to the kinematic control of rolling rovers [53,54].

The robot geometrical and inertial properties used in this work are the ones of the robotic arm used for the experimental validation of the LS-based IK solution in the 2D fixed base case [23]. This planar robot is derived from the 3D free-floating robot used in the Parabolic Flight tests performed by one of the authors [26,55-60], in which the IK solution proposed by Caccavale and Siciliano [5] was implemented and tested. Similarly, the floating base geometrical and inertial properties considered in this study are the ones of the aforementioned free-floating robot.

In this paper, two novel methods are proposed and compared for capturing a non-cooperative target with a redundant robot and in the meantime transferring a null reaction torque to the base spacecraft. This is a great advantage with respect to the state of the art capture methods, in which the problem of capture and of reactions minimization are handled separately and their integration is not straightforward. In the first method, the end-effector follows a parametric trajectory, which parameters are computed in order to have the same direction and speed of the target at the time of capture. On the other hand, in the second method the end-effector trajectory is computed by making the position and velocity error converge to zero inside the inverse kinematics control loop. The

proposed methods have been demonstrated and compared by means of dynamic simulations of a 3-DOF planar manipulator. Both of them have shown a good performance and in particular in both cases the manipulator is able to reach the target with the desired end-effector velocity and with a null reaction torque transferred to the base spacecraft.

LEAST-SQUARES-BASED REACTION CONTROL SOLUTION

In this Section, some concepts are recalled on the LS-based reaction control solution presented in [15] and [19] which are useful for the purposes of this work.

Consider a redundant n-DOF space manipulator which has to track k components of the end-effector pose. The degree of redundancy of the manipulator is $r = n - k > 1$ and, if r is equal to the number of reaction torque components to be minimized, it is possible to study the existence of a zero torque IK solution. In order to minimize the base reaction torque, the redundancy should be solved at the acceleration level and, therefore, the Forward Kinematics equation can be expressed as:

$$\boldsymbol{J}\ddot{\boldsymbol{q}} + \dot{\boldsymbol{J}}\dot{\boldsymbol{q}} - \ddot{\boldsymbol{x}} = \boldsymbol{0} \tag{1}$$

in which $\ddot{\boldsymbol{x}}$ represents the desired end-effector acceleration, $\dot{\boldsymbol{q}}, \ddot{\boldsymbol{q}}$ are the joint velocities and accelerations, and $\boldsymbol{J}, \dot{\boldsymbol{J}}$ are the manipulator *Generalized Jacobian Matrix* [61] and its time derivative. For redundant manipulators Eq. (1) is undetermined since $k < n$.

If a desired end-effector acceleration vector $\ddot{\boldsymbol{x}}$ is given, and current $\boldsymbol{q}$ and $\dot{\boldsymbol{q}}$ are known, Eq. (1) can be solved by means of the pseudoinverse of the Generalized Jacobian Matrix:

$$\ddot{\boldsymbol{q}} = \boldsymbol{J}^{\dagger}(\ddot{\boldsymbol{x}} - \dot{\boldsymbol{J}}\dot{\boldsymbol{q}}) + (\boldsymbol{I} - \boldsymbol{J}^{\dagger}\boldsymbol{J})\ddot{\boldsymbol{\phi}} \tag{2}$$

The first term in the right-hand side of Eq. (2) stands for the classical *pseudoinverse solution*, which is the particular solution that minimizes $\|\ddot{\boldsymbol{q}}\|$, whereas the second term represents the general solution of the homogeneous system $\boldsymbol{J}\ddot{\boldsymbol{q}} = \boldsymbol{0}$. Different $\ddot{\boldsymbol{q}}$ can be generated for the same $\ddot{\boldsymbol{x}}$ by varying the vector $\ddot{\boldsymbol{\phi}}$ arbitrarily and projecting it onto the null-space of $\boldsymbol{J}$ by means of the projecting operator $(\boldsymbol{I} - \boldsymbol{J}^{\dagger}\boldsymbol{J})$, where $\boldsymbol{I}$ is the identity matrix.

The *pseudoinverse solution*, which is also called *LS solution*, can be used as a reference in order to measure the performance of the solution which minimizes the reaction torque, as proposed in [24].

On the other hand, the reaction torque about the spacecraft center of mass can be expressed as [10]:

$$\boldsymbol{T} = \boldsymbol{M}\ddot{\boldsymbol{q}} + \boldsymbol{n} \tag{3}$$

in which the mass matrix $\boldsymbol{M}$ depends on the joint variables of the manipulator $\boldsymbol{q}$, and the centrifugal and Coriolis term $\boldsymbol{n}$ depends on $\boldsymbol{q}$ and $\dot{\boldsymbol{q}}$.

A suitable measure for the base reaction torque is represented by the quadratic cost function:

$$f(\ddot{\boldsymbol{q}}) = \boldsymbol{T}^{\mathrm{T}}\boldsymbol{T} = \|\boldsymbol{T}\|^2 \tag{4}$$

which depends on $\ddot{\boldsymbol{q}}$ only, since the current $\boldsymbol{q}$ and $\dot{\boldsymbol{q}}$ are considered as state variables.

In this context, the following local constrained optimization problem can be defined:

$$\begin{aligned} &\text{Min } f(\ddot{\boldsymbol{q}}) = \boldsymbol{T}^{\mathrm{T}}\boldsymbol{T} \\ &\text{subject to } \boldsymbol{J}\ddot{\boldsymbol{q}} + \dot{\boldsymbol{J}}\dot{\boldsymbol{q}} - \ddot{\boldsymbol{x}} = \boldsymbol{0} \end{aligned} \tag{5}$$

in which $\ddot{\boldsymbol{q}}$ represents the local optimization variable.

The base reaction torque $\boldsymbol{T}$ depends linearly on $\ddot{\boldsymbol{q}}$, Eq. (3), since the current $\boldsymbol{q}$ and $\dot{\boldsymbol{q}}$ are considered as state variables. Equation (5) can be therefore interpreted as the formulation of a linear *Least Squares problem with Equality constraints* (LSE) [23,62] in the $\ddot{\boldsymbol{q}}$ unknown.

A closed-form solution can be found for the LSE problem by combining Eqs. (2) and (3) [23,62]:

$$\begin{aligned} \ddot{\boldsymbol{q}} = &\boldsymbol{J}^{\dagger}(\ddot{\boldsymbol{x}} - \dot{\boldsymbol{J}}\dot{\boldsymbol{q}}) + \\ &-[\boldsymbol{M}(\boldsymbol{I} - \boldsymbol{J}^{\dagger}\boldsymbol{J})]^{\dagger}[\boldsymbol{M}\boldsymbol{J}^{\dagger}(\ddot{\boldsymbol{x}} - \dot{\boldsymbol{J}}\dot{\boldsymbol{q}}) + \boldsymbol{n}] \end{aligned} \tag{6}$$

The solution presented in this section, and its extension which takes into account the joint acceleration limits, result to be suitable for real-time implementation by means of recursive algorithms [33], by means of solution techniques used for the more general constrained Quadratic Programming problem [34-38], or by means of neural networks algorithms [29,39-41]. Moreover, if a LS routine is available on the onboard computer, this can be used to solve the LSE problem by implementing the weighting method due to Van Loan [62-64].

A useful generalization of the constrained optimization problem of Eq. (5) can be made by introducing inequality constraints on joint accelerations:

$$\text{Min } f(\ddot{\boldsymbol{q}}) = \boldsymbol{T}^{\mathrm{T}}\boldsymbol{T} \qquad \text{subject to } \begin{cases} \boldsymbol{J}\ddot{\boldsymbol{q}} + \dot{\boldsymbol{J}}\dot{\boldsymbol{q}} - \ddot{\boldsymbol{x}} = \boldsymbol{0} \\ \overline{\ddot{\boldsymbol{q}}}_l \le \ddot{\boldsymbol{q}} \le \overline{\ddot{\boldsymbol{q}}}_u \end{cases} \tag{7}$$

in which $\overline{\ddot{\boldsymbol{q}}}_l, \overline{\ddot{\boldsymbol{q}}}_u$ represent the lower and upper acceleration limits, respectively. The inequalities are interpreted componentwise, and the joint acceleration limits may in general be different for each robot joint. This formulation leads to the minimization of the base reaction torque and in the meantime to the limitation of joint accelerations under physically acceptable values. In particular, this formulation has the advantage that the avoidance of algorithmic instabilities [31,32] may be automatically fulfilled.

Similarly to the LSE case, the constrained optimization problem of Eq. (7) can be interpreted as the formulation of a linear *Least Squares problem with Equality and Inequality constraints* (LSEI) [23,62] in the $\ddot{\boldsymbol{q}}$ unknown.

The presence of inequality constraints makes it not possible to obtain a closed-form solution in this case. Nevertheless, the algorithms for the real-time solution of the LSE problem have been developed (or modified) in order to be also suitable for the solution of the LSEI problem [29,33-41].

The theory presented in this section has been written considering the base reaction torques minimization. Nevertheless, it can be straightforwardly extended to the minimization of the base reaction forces and of weighted combinations of base reaction torques and forces, such as presented in [15].

CAPTURE METHODS AND SIMULATED RESULTS

Parametric-trajectory reactionless capture method

In the first capture method, which we will refer to as "Parametric-trajectory reactionless capture method", the LSE method is used, with a parametric half circle trajectory for the robot end-effector.

The parametric information (radius, center, curvilinear abscissa) are computed from the target information (initial position, direction, velocity), in such a way that:

- the target is captured in the point of its trajectory with minimum distance with respect to the end-effector initial position;

- the end-effector trajectory is tangent to the target trajectory at the time of capture;

- the end-effector velocity is the same as the target velocity at the time of capture;

- the curvilinear abscissa is derived (by integration) from a curvilinear acceleration profile which is a combination of cosine functions (in order to have a sufficiently smooth curvilinear abscissa, i.e. to be continuous with continuous derivative up to its 2nd order derivative, see for example Figs. 2-4).

Two target trajectories will be tested in order to show the performance and reliability of the capture method, which works for whatever target trajectory, with the obvious exception of the cases in which some kinematic or dynamic singularities of the manipulator are encountered (which anyway can be avoided by using standard singularity avoidance methods):

- Target trajectory 1): target approaching with a 45° angle with respect to the Ox axis of the manipulator (see Fig. 1).

- Target trajectory 2): target approaching with a 0° angle with respect to the Ox axis of the manipulator.

The target velocity is set to 0.1 m/s in both cases.

Target trajectory 1)

In Fig. 1 (top) a stroboscopic view of the robotic capture is presented, together with the plot of the reaction torque (bottom), which is always null with some negligible numerical noise.

In Figs. 2-4 the plot of the curvilinear abscissa and its first and second derivatives are presented.

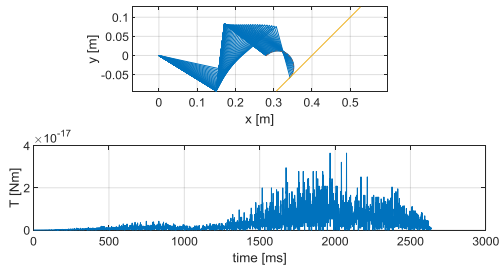

Figure 1. Stroboscopic view of robot motion (top), and reaction torque (bottom) – Parametric trajectory, trajectory 1).

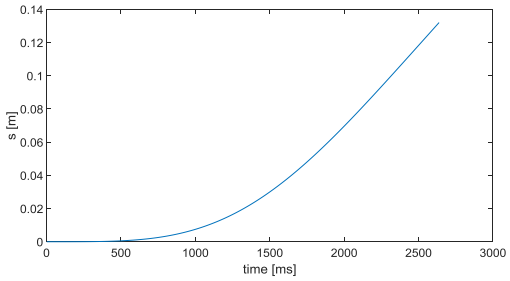

Figure 2. Curvilinear abscissa – Parametric trajectory, trajectory 1).

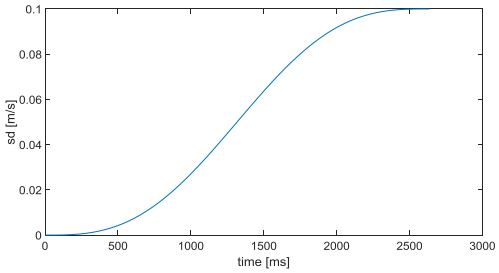

Figure 3. First derivative of curvilinear abscissa – Parametric trajectory, trajectory 1).

In Figs. 5-7 the plot of joint angles, velocities, and accelerations are presented.

In Fig. 8 the plot of the error between the end-effector and the target is presented.

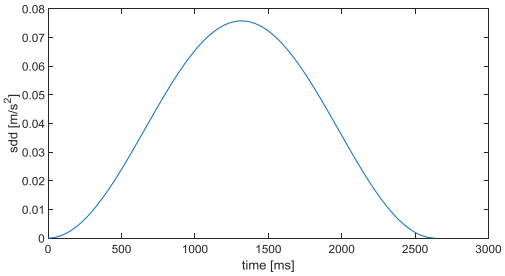

Figure 4. Second derivative of curvilinear abscissa – Parametric trajectory, trajectory 1).

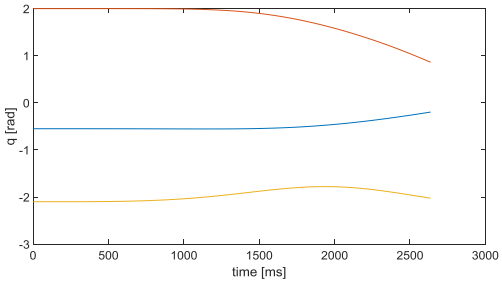

Figure 5. Joint angles - Parametric trajectory, trajectory 1).

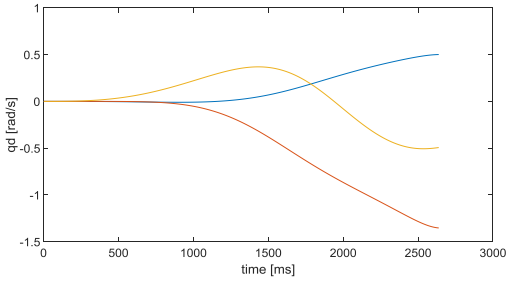

Figure 6. Joint velocities - Parametric trajectory, trajectory 1).

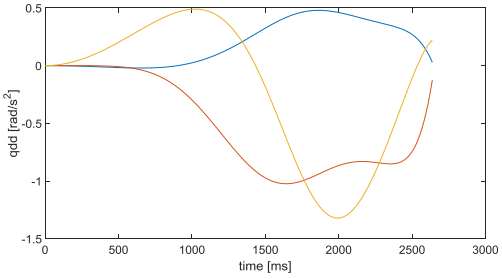

Figure 7. Joint accelerations - Parametric trajectory, trajectory 1).

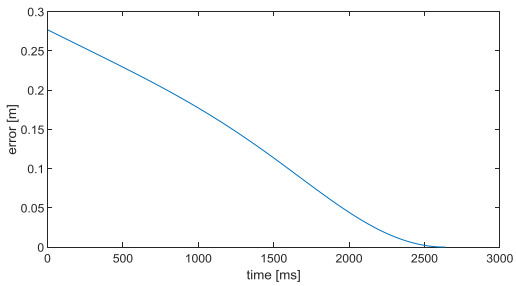

Figure 8. Capture error - Parametric trajectory, trajectory 1).

Target trajectory 2)

In Fig. 9 (top) a stroboscopic view of the robotic capture is presented, together with the plot of the reaction torque (bottom), which is always null with some negligible numerical noise.

In Figs. 10-12 the plot of the curvilinear abscissa and its first and second derivatives are presented.

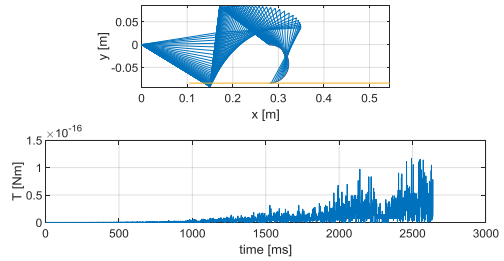

Figure 9. Stroboscopic view of robot motion (top), and reaction torque (bottom) – Parametric trajectory, trajectory 2).

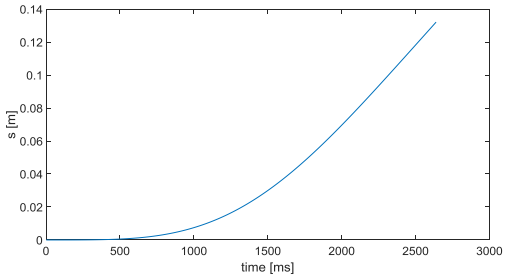

Figure 10. Curvilinear abscissa – Parametric trajectory, trajectory 2).

In Figs. 13-15 the plot of joint angles, velocities, and accelerations are presented.

In Fig. 16 the plot of the error between the end-effector and the target is presented.

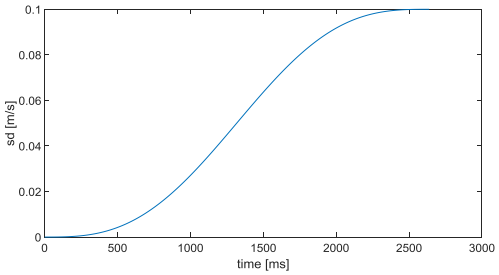

Figure 11. First derivative of curvilinear abscissa – Parametric trajectory, trajectory 2).

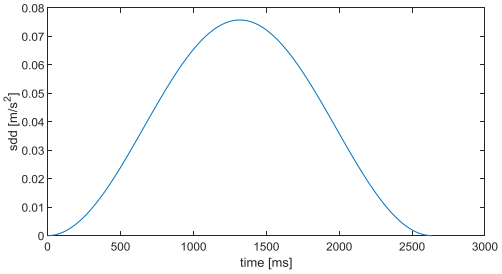

Figure 12. Second derivative of curvilinear abscissa – Parametric trajectory, trajectory 2).

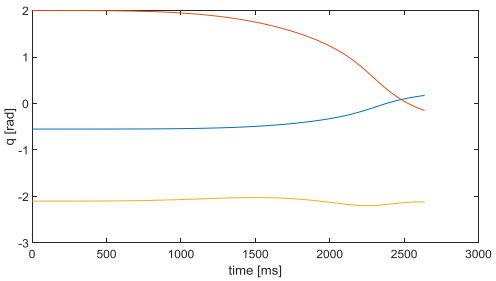

Figure 13. Joint angles - Parametric trajectory, trajectory 2).

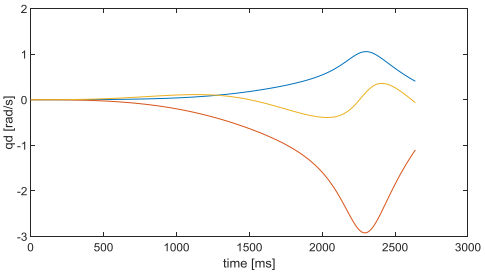

Figure 14. Joint velocities - Parametric trajectory, trajectory 2).

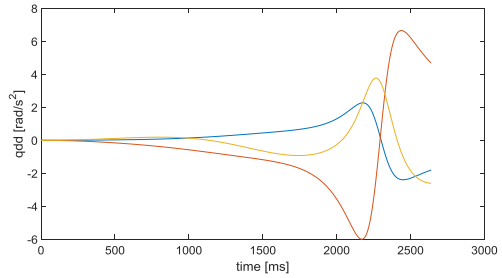

Figure 15. Joint accelerations - Parametric trajectory, trajectory 2).

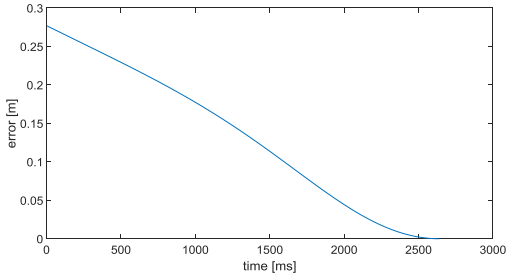

Figure 16. Capture error - Parametric trajectory, trajectory 2).

Free-shape-trajectory reactionless capture method

In the second capture method, which we will refer to as "Free-shape-trajectory reactionless capture method", the LSE method is used, and the end-effector trajectory is computed by double integration of the $\ddot{\boldsymbol{x}}$, where the position error (**e**) and velocity error (d**e**/dt) are reduced to zero by means of two gains k_p and k_d, such that:

$$\ddot{\boldsymbol{x}}_d = \ddot{\boldsymbol{x}} - k_p * \mathbf{e} - k_d * d\mathbf{e}/dt \qquad (8)$$

where $\ddot{\boldsymbol{x}}_d$ is the desired end-effector acceleration, and $\ddot{\boldsymbol{x}}$ is the current end-effector acceleration.

In this case, both the end-effector trajectory and the curvilinear abscissa are not fixed in advance (such as it was in the Parametric-trajectory reactionless capture method) but they are computed by the kinematic inversion algorithm.

Similarly to the previous capture method, the same two target trajectories of the previous case will be used (with also the same target initial position and velocity) in order to demonstrate the capture method and compare the results. Also the robot model and initial configuration are the same as used in the previous capture method.

As it can be easily verified in the Figs. 17-32 below, using the gains k_p = 7.7 and k_d = 5 (which work correctly in all the robot workspace), the target is always reached (**e** → **0** and d**e**/dt → **0**), and in particular the speed and direction of the end-effector are equal to the ones of the target at the time of capture, avoiding undesired impact forces.

Target trajectory 1)

In Fig. 17 (top) a stroboscopic view of the robotic capture is presented, together with the plot of the reaction torque (bottom), which is always null with some negligible numerical noise.

In Figs. 18-20 the plot of the curvilinear abscissa and its first and second derivatives are presented.

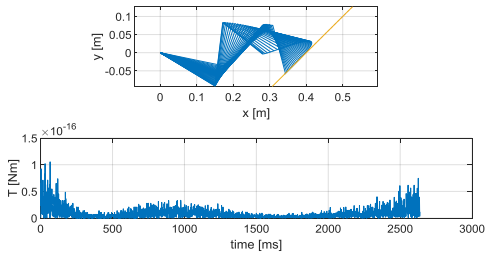

Figure 17. Stroboscopic view of robot motion (top), and reaction torque (bottom) – Free shape trajectory, trajectory 1).

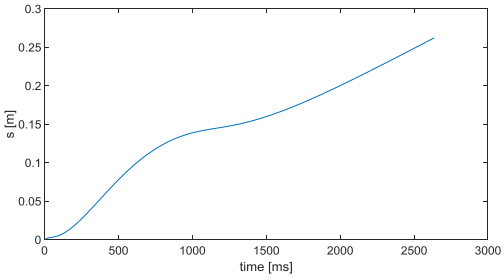

Figure 18. Curvilinear abscissa – Free shape trajectory, trajectory 1).

In Figs. 21-23 the plot of joint angles, velocities, and accelerations are presented.

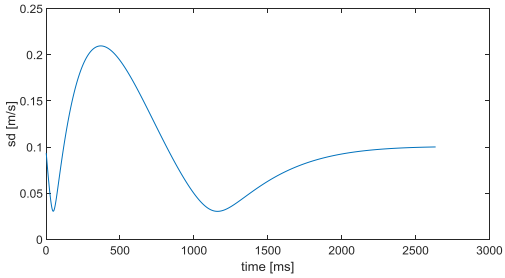

Figure 19. First derivative of curvilinear abscissa – Free shape trajectory, trajectory 1).

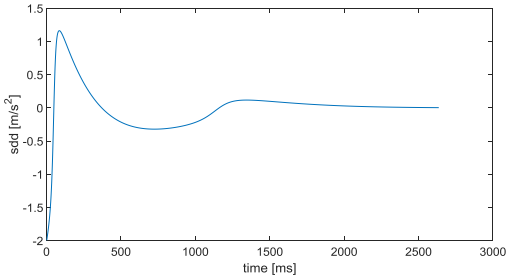

Figure 20. Second derivative of curvilinear abscissa – Free shape trajectory, trajectory 1).

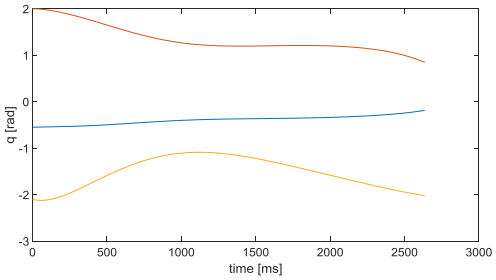

Figure 21. Joint angles - Free shape trajectory, trajectory 1).

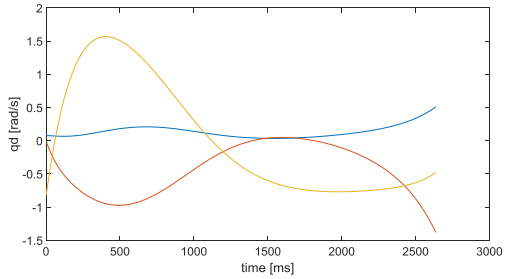

Figure 22. Joint velocities - Free shape trajectory, trajectory 1).

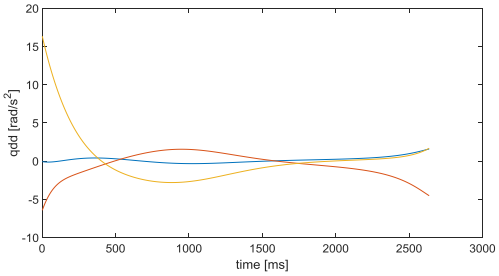

Figure 23. Joint accelerations - Free shape trajectory, trajectory 1).

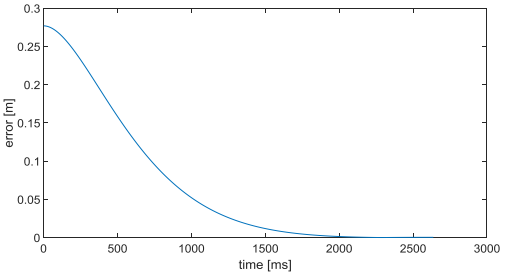

Figure 24. Capture error - Free shape trajectory, trajectory 1).

In Fig. 24 the plot of the error between the end-effector and the target is presented.

Target trajectory 2)

In Fig. 25 (top) a stroboscopic view of the robotic capture is presented, together with the plot of the reaction torque (bottom), which is always null with some negligible numerical noise.

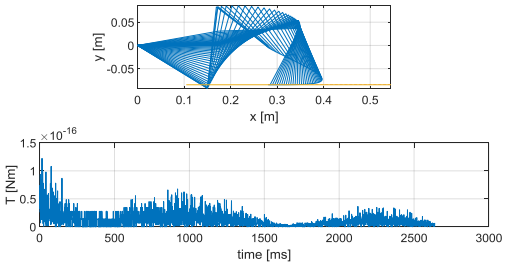

Figure 25. Stroboscopic view of robot motion (top), and reaction torque (bottom) – Free shape trajectory, trajectory 2).

In Figs. 26-28 the plot of the curvilinear abscissa and its first and second derivatives are presented.

In Figs. 29-31 the plot of joint angles, velocities, and accelerations are presented.

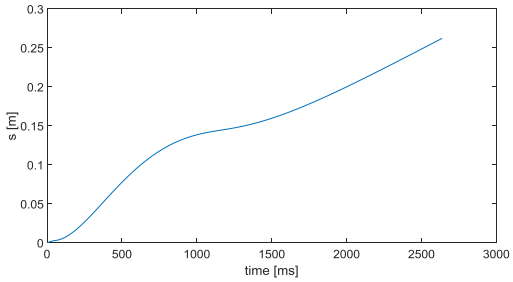

Figure 26. Curvilinear abscissa – Free shape trajectory, trajectory 2).

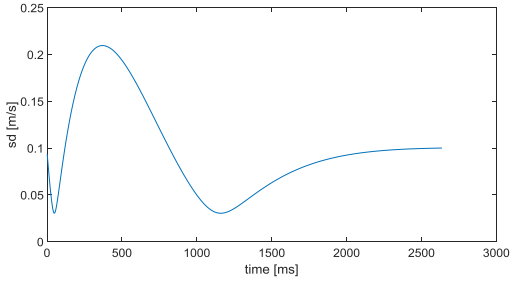

Figure 27. First derivative of curvilinear abscissa – Free shape trajectory, trajectory 2).

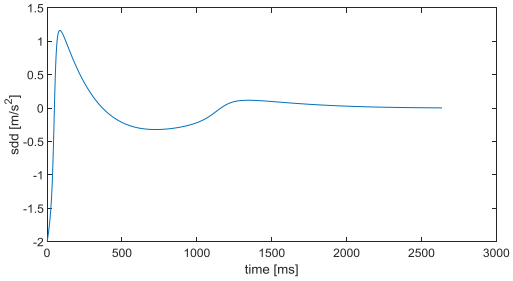

Figure 28. Second derivative of curvilinear abscissa – Free shape trajectory, trajectory 2).

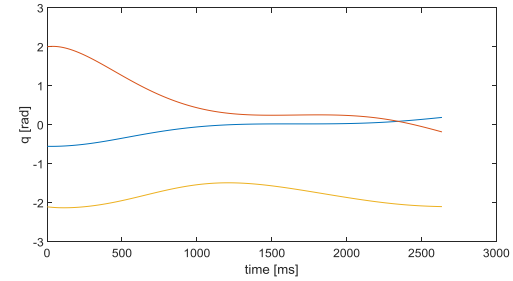

Figure 29. Joint angles - Free shape trajectory, trajectory 2).

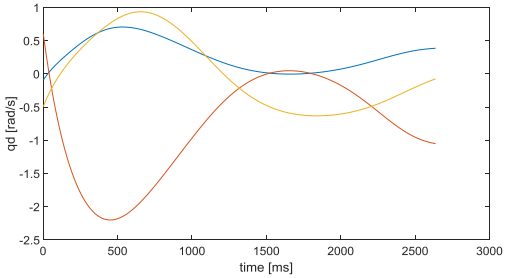

Figure 30. Joint velocities - Free shape trajectory, trajectory 2).

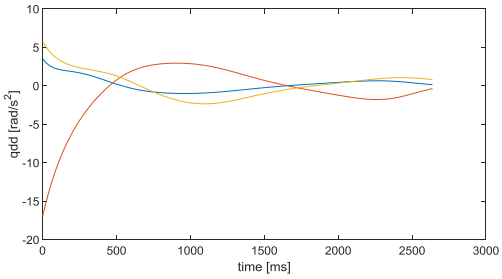

Figure 31. Joint accelerations - Free shape trajectory, trajectory 2).

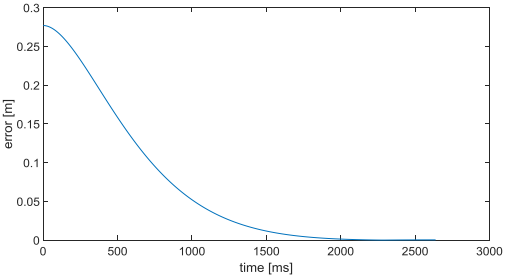

Figure 32. Capture error - Free shape trajectory, trajectory 2).

In Fig. 32 the plot of the error between the end-effector and the target is presented.

Comparison of the two capture methods

In the dynamic simulations both the presented methods have shown a good performance. In particular, the end-effector reaches the target with a zero relative velocity and with a tangent trajectory to the one of the target (which assures that no impact force is exchanged during the capture) and, moreover, the reaction torque transferred to the spacecraft base is always null in both cases.

As it can be verified in Figs. 5-7, 13-15, 21-23, 29-31, the joint angle, velocity, and acceleration profiles are feasible for both methods.

From the comparison of Figs. 8 and 24, and 16 and 32 it can be noticed that the position error converges to zero much more quickly with the Free-shape-trajectory reactionless capture, and therefore the capture position is also anticipated, such as it can be easily verified in the stroboscopic views of robot motion (compare Figs. 1 and 17, and 9 and 25). This is an important advantage, since more time is available to track the target and correct eventual position errors.

On the other hand, the Free-shape-trajectory reactionless capture:

a) has not null joint velocities and accelerations at the starting point (see Figs. 22,23 and 30,31), which can be easily solved with a blend with a smoother solution at the beginning of the trajectory;

b) needs a longer curvilinear abscissa to reach the target (compare Figs. 2 and 18, and 10 and 26), which is related to slightly higher joint velocities and accelerations with respect to the Parametric-trajectory reactionless capture method (compare Figs. (6,22), (7,23), (14,30), and (15,31));

c) exhibits some overshoots in the derivatives of the curvilinear abscissa (see Figs. 19,20 and 27,28), which are due to the nonlinearity of the robot dynamic model, and a method to reduce them could be part of future work.

It can be also noticed that c) most probably is the cause of b).

Concluding, the Free-shape-trajectory reactionless capture demonstrates to capture the target quickly and with anticipated capture positions. Nevertheless, considered its drawbacks (even if of limited importance and easily solvable, such as the overshoots and slightly higher joint velocities and accelerations), one can choose the most suitable capture method depending on the operations requirements.

CONCLUSIONS

In this paper, two novel methods are proposed and compared for capturing a non-cooperative target with a redundant robot and in the meantime transferring a null reaction torque to the base spacecraft. This is a great advantage with respect to the state of the art capture methods, in which the problem of capture and of reactions minimization are handled separately and their integration is not straightforward. In the first method, the robot end-effector follows a parametric trajectory, which parameters are computed in order to have the same direction and speed of the target at the time of capture. On the other hand, in the second method the end-effector trajectory is computed by making the position and velocity error converge to zero inside the inverse kinematics control loop. In the dynamic simulations both the presented methods have shown a good performance: the end-effector reaches the target with a zero relative velocity and with a tangent trajectory to the one of the target (which assures that no impact force is exchanged during the capture) and, moreover, the reaction torque transferred to the spacecraft base is always null in both cases. Finally, the Free-shape-trajectory reactionless capture demonstrates to capture the target quickly and with anticipated capture positions. Nevertheless, it has some limited and easily solvable drawbacks, such as some overshoots and slightly higher joint velocities and accelerations, and therefore one can choose the most suitable capture method depending on the operations requirements. The development, test, and validation of a 3D robot prototype using the proposed capture methods will be part of future work.

REFERENCES

[1] Dubowsky, S., Papadopoulos, E., “The Kinematics, Dynamics, and Control of Free-Flying and Free-Floating Space Robotic Systems,” IEEE Transactions on Robotics and Automation, Vol. 9, No. 5, 1993, pp. 531–543.

[2] Oda, M., "Attitude Control Experiments of a Robot Satellite," Journal of Spacecraft and Rockets, Vol. 37, No. 6, 2000, pp. 788–794.

[3] Yoshida, K., "Engineering Test Satellite VII Flight Experiments for Space Robot Dynamics and Control: Theories on Laboratory Test Beds Ten Years Ago, Now in Orbit," International Journal of Robotics Research, Vol. 22, No. 5, 2003, pp. 321–335.

[4] Nenchev, D., Umetani, Y., Yoshida, K., "Analysis of a Redundant Free-Flying Spacecraft/Manipulator System," IEEE Transactions on Robotics and Automation, Vol. 8, No. 1, 1992, pp. 1–6.

[5] Caccavale, F., Siciliano, B., "Kinematic Control of Redundant Free-Floating Robotic Systems," Advanced Robotics, Vol. 15, No. 4, 2001, pp. 429–448.

[6] Nenchev, D., Yoshida, K., Umetani, Y., "Analysis, Design and Control of Free-Flying Space Robots Using Fixed-Attitude-Restricted Jacobian Matrix," 5th International Symposium on Robotics Research, edited by H. Miura and S. Arimoto, MIT Press, Cambridge, MA, 1991, pp. 251–258.

[7] Dubowsky, S., Torres, M. A., "Path Planning for Space Manipulators to Minimize Spacecraft Attitude Disturbances," 1991 IEEE International Conference on Robotics and Automation, Sacramento, CA, Vol. 3, 1991, pp. 2522–2528.

[8] Torres, M. A., Dubowsky, S., "Minimizing Spacecraft Attitude Disturbances in Space Manipulator Systems," Journal of Guidance, Control, and Dynamics, Vol. 15, No. 4, 1992, pp. 1010–1017.

[9] De Silva, C. W., "Trajectory Design for Robotic Manipulators in Space Applications," Journal of Guidance, Control, and Dynamics, Vol. 14, No. 3, 1994, pp. 670–674.

[10] Quinn, R. D., Chen, L., Lawrence, C., "Base Reaction Control for Space-Based Robots Operating in Microgravity Environment," Journal of Guidance, Control, and Dynamics, Vol. 17, No. 2, 1994, pp. 263–270.

[11] Shäfer, B., Krenn, R., Rebele, B., "On Inverse Kinematics and Kinetics of Redundant Space Manipulator Simulation," Journal of Computational and Applied Mechanics, Vol. 4, No. 1, 2003, pp. 53–70.

[12] Krenn, R., Hirzinger, G. "Modular, Generic Inverse Kinematics Algorithm Applied to Kinematically Redundant Space Manipulators," 8th ESA Workshop on Advanced Space Technologies for Robotics and Automation, Noordwijk, The Netherlands, 2004.

[13] Nenchev, D. N., Yoshida, K., Vichitkulsawat, P., "Reaction Null-Space Control of Flexible Structure Mounted Manipulator Systems," IEEE Transactions on Robotics and Automation, Vol. 15, No. 6, 1999, pp. 1011–1023.

[14] Yoshida, K., Nenchev, D. N., Uchiyama, M., "Moving Base Robotics and Reaction Management Control," 7th International Symposium on Robotics Research, edited by G. Giralt and G. Hirzinger, Springer-Verlag, Berlin, Germany, 1996, pp. 101–109.

[15] Cocuzza, S., Pretto, I., Debei, S., "Least-squares-based reaction control of space manipulators," Journal of Guidance, Control, and Dynamics, Vol. 35, no. 3, 2012, pp. 976-986.

[16] Cocuzza, S., Pretto, I., Debei, S., "Novel reaction control techniques for redundant space manipulators: Theory and simulated microgravity tests," Acta Astronautica, Vol. 68, No. 11-12, 2011, pp. 1712-1721.

[17] Cocuzza, S., Artusi, M., Debei, S., "Zero reaction workspace of a space manipulator," 61st International Astronautical Congress 2010, IAC 2010, Vol. 11, pp. 8834-8845, 2010.

[18] Cocuzza, S., Pretto, I., Debei, S., "Dynamic control of redundant space manipulators suitable for real-time applications," 61st International Astronautical Congress 2010, IAC 2010, Vol. 4, pp. 3332-3345, 2010.

[19] Cocuzza, S., Pretto, I., Debei, S., "Reaction torque control of redundant space robotic systems for orbital maintenance and simulated microgravity

tests," Acta Astronautica, Vol. 67, No. 3-4, 2010, pp. 285-295.
[20] Cocuzza, S., Pretto, I., Debei, S., "Novel reaction control techniques for redundant space manipulators: Theory and simulated microgravity tests," 60th International Astronautical Congress 2009, IAC 2009, Vol. 1, pp. 827-841, 2009.
[21] Cocuzza, S., Pretto, I., Debei, S., "A constrained least squares approach for reaction torque control in spacecraft/manipulator systems," 60th International Astronautical Congress 2009, IAC 2009, Vol. 6, pp. 4957-4968, 2009.
[22] Pretto, I., Cocuzza, S., Debei, S., "Dynamic coordination principles for multiple spacecraft mounted manipulators," 60th International Astronautical Congress 2009, IAC 2009, Vol. 9, pp. 7029-7038, 2009.
[23] Cocuzza, S., Pretto, I., Angrilli, F., "Optimal kinematic control of redundant space robotic systems for orbital maintenance: Simulated microgravity tests," International Astronautical Federation - 59th International Astronautical Congress 2008, IAC 2008, Vol. 1, pp. 601-614, 2008.
[24] Cocuzza, S., Pretto, I., Menon, C., Angrilli, F., "Control of dynamic attitude disturbances on spacecrafts equipped with robotic systems for orbital maintenance," International Astronautical Federation - 58th International Astronautical Congress 2007, Vol. 7, pp. 4641-4649, 2007.
[25] Alexander, H. L., Cannon, R. H., "An Extended Operational-Space Control Algorithm for Satellite Manipulators," The Journal of the Astronautical Sciences, Vol. 38, No. 4, 1990, pp. 473–486.
[26] Cocuzza, S., "Design and Construction of a Free-Flying 3D Robot for Space Applications and Microgravity Tests," Ph.D. Thesis, CISAS "G. Colombo" - Center of Studies and Activities for Space, University of Padova, Italy, 2005.
[27] Cocuzza, S., Menon, C., Angrilli, F., "Free-flying robot tested on ESA parabolic flights: Simulated microgravity tests and simulator validation," International Astronautical Federation - 58th International Astronautical Congress 2007, Vol. 1, pp. 593-608, 2007.
[28] Cocuzza, S., Bettanini, C., De Cecco, M., Menon, C., Zaccariotto, M., Angrilli, F., "Free-flying robot 3D simulator validation by means of air-bearings table 2D tests - Test-bed design," International Astronautical Federation - 56th International Astronautical Congress 2005, Vol. 5, pp. 3472-3485, 2005.
[29] Zhang, Y., Wang, J., Xia, Y., "A Dual Neural Network for Redundancy Resolution of Kinematically Redundant Manipulators Subject to Joint Limits and Joint Velocity Limits," IEEE Transactions on Neural Networks, Vol. 14, No. 3, 2003, pp. 658–667.
[30] Zhang, Y., Wang, J., "Obstacle Avoidance for Kinematically Redundant Manipulators Using a Dual Neural Network," IEEE Transactions on Systems, Man, and Cybernetics, Part B, Vol. 34, No. 1, 2004, pp. 752–759.
[31] O'Neil, K. A., Divergence of Linear Acceleration-Based Redundancy Resolution Schemes," IEEE Transactions on Robotics and Automation, Vol. 18, No. 4, 2002, pp. 625–631.
[32] Park, J., Chung, W. K., Youm, Y., "Characterization of Instability of Dynamic Control for Kinematically Redundant Manipulators," IEEE International Conference on Robotics and Automation, Vol. 3, 2002, pp. 2400–2405.
[33] Zhu, Y., Li, X. R., "Recursive Least Squares with Linear Constraints," 38th IEEE Conference on Decision and Control, Phoenix, AZ, Vol. 3, 1999, pp. 2414–2419.
[34] Park, K. C., Chang, P. H., Kim, S. H., "The Enhanced Compact QP Method for Redundant Manipulators Using Practical Inequality Constraints," 1998 IEEE International Conference on Robotics and Automation, Leuven, Belgium, Vol. 1, 1998, pp. 107–114.
[35] Cheng, F. T., Sheu, R. J., Chen, T. H., "The Improved Compact QP Method for Resolving Manipulator Redundancy," IEEE Transactions on

Systems, Man, and Cybernetics, Vol. 25, No. 11, 1995, pp. 1521–1530.
[36] Cheng, F. T., Chen, T. H., Sun Y. Y., "Resolving Manipulator Redundancy Under Inequality Constraints," IEEE Transactions on Robotics and Automation, Vol. 10, No. 1, 1994, pp. 65–71.
[37] Zhang, Y., Ma, S., "Minimum-Energy Redundancy Resolution of Robot Manipulators Unified by Quadratic Programming and its Online Solution," 2007 IEEE International Conference of Mechatronics and Automation, Harbin, China, 2007, pp. 3232–3237.
[38] Xu, J. X., Wang, W., "Two Optimization Algorithm for Solving Robotics Inverse Kinematics with Redundancy," 2007 IEEE International Conference on Control and Automation, Guangzhou, China, 2007, pp. 3021–3028.
[39] Zhang, Y., Wang, J., "A Dual Neural Network for Convex Quadratic Programming Subject to Linear Equality and Inequality Constraints," Physics Letters A, Vol. 298, 2002, pp. 271–278.
[40] Zhang, Y., Ge, S. S., Lee, T. H., "A Unified Quadratic-Programming-Based Dynamical System Approach to Joint Torque Optimization of Physically Constrained Redundant Manipulators," IEEE Transactions on Systems, Man, and Cybernetics, Part B, Vol. 34, No. 5, 2004, pp. 2126–2132.
[41] Xia, Y. S., Feng, G., Wang, J., "A Primal-Dual Neural Network for Online Resolving Constrained Kinematic Redundancy in Robot Motion Control," IEEE Transactions on Systems, Man, and Cybernetics, Part B, Vol. 35, No. 1, 2005, pp. 54–64.
[42] Cocuzza, S., Chiaradia, M., Debei, S., "Dynamic coordination of a multi-DOF manipulator-platform system," 63rd International Astronautical Congress 2012, IAC 2012, Naples, Italy, 2012.
[43] Cocuzza, S., Chiaradia, M., Debei, S., "Base reaction control of hyper-redundant space manipulators," 62nd International Astronautical Congress 2011, IAC 2011, Vol. 7, pp. 5571-5581, 2011.
[44] Chiaradia, M., Cocuzza, S., Debei, S., "Increased performance reaction control of multi degrees of freedom space manipulators," 62nd International Astronautical Congress 2011, IAC 2011, Vol. 8, pp. 6896-6906, 2011.
[45] Cocuzza, S., Zampierin, S., Debei, S., "Zero reaction workspace in the operations of multi degrees of freedom space manipulators for orbital maintenance," 63rd International Astronautical Congress 2012, IAC 2012, Naples, Italy, 2012.
[46] Zampierin, S., Cocuzza, S., Debei, S., "Reaction control of multi degrees of freedom space manipulators: theory and simulated microgravity tests," 63rd International Astronautical Congress 2012, IAC 2012, Naples, Italy, 2012.
[47] Correnti, A., Cocuzza, S., Debei, S., "Augmented workspace of a multi-DOF space manipulator for reactionless target capture," 64th International Astronautical Congress 2013, IAC 2013, Beijing, China, 2013.
[48] Cocuzza, S., Cuccato, D., Debei, S., "Least-squares-based reactionless capture of a non-cooperative spacecraft with a space manipulator," 64th International Astronautical Congress 2013, IAC 2013, Beijing, China, 2013.
[49] Cocuzza, S., Rossi, S., Debei, S., "Novel reaction control of space manipulators with increased robustness against singularities and physical joint limits," 63rd International Astronautical Congress 2012, IAC 2012, Naples, Italy, 2012.
[50] Cocuzza, S., Rossi, S., Debei, S., "Robust reaction control of space manipulators," 62nd International Astronautical Congress 2011, IAC 2011, Vol. 1, pp. 627-639, 2011.
[51] Rossi, S., Cocuzza, S., Debei, S., "Novel strategies to increase robustness in the reaction control of space manipulators," 62nd International Astronautical Congress 2011, IAC 2011, Vol. 6, pp. 5111-5123, 2011.
[52] Pretto, I., Ruffieux, S., Menon, C., Ijspeert, A.J., Cocuzza, S., "A Point-Wise Model of Adhesion Suitable for Real-Time Applications of Bio-Inspired

Climbing Robots," Journal of Bionic Engineering, Vol. 5 (SUPPL.), 2008, pp. 98-105.
[53] Artusi, M., Potz, M., Aristiźabal, J., Menon, C., Cocuzza, S., Debei, S., "Electroactive elastomeric actuators for the implementation of a deformable spherical rover," IEEE/ASME Transactions on Mechatronics, art. no. 5680664, Vol. 16, No. 1, 2011, pp. 50-57.
[54] Potz, M., Artusi, M., Soleimani, M., Menon, C., Cocuzza, S., Debei, S., "Rolling dielectric elastomer actuator with bulged cylindrical shape," Smart Materials and Structures, art. no. 127001, Vol. 19, No. 12, 2010.
[55] Cocuzza, S., Menon, C., Aboudan, A., Bulgarelli, A., Angrilli, F., "Free-flying 3D space robot prototype design and Zero-G experiments on ESA parabolic flights," International Astronautical Federation - 55th International Astronautical Congress 2004, Vol. 4, pp. 2252-2261, 2004.
[56] Menon, C., Busolo, S., Cocuzza, S., Aboudan, A., Bulgarelli, A., Bettanini, C., Marchesi, M., Angrilli, F., "Issues and solutions for testing free-flying robots," Acta Astronautica, Vol. 60, No. 12, 2007, pp. 957-965.
[57] Menon, C., Aboudan, A., Cocuzza, S., Bulgarelli, A., Angrilli, F., "Free-flying robot tested on parabolic flights: Kinematic control," Journal of Guidance, Control, and Dynamics, Vol. 28, No. 4, 2005, pp. 623-630.
[58] Menon, C., Busolo, S., Cocuzza, S., Aboudan, A., Bulgarelli, A., Bettanini, C., Angrilli, F., "Issues and new solutions for testing free-flying robots," International Astronautical Federation - 55th International Astronautical Congress 2004, Vol. 8, pp. 5048-5058, 2004.
[59] Menon, C., Aboudan, A., Cocuzza, S., Bulgarelli, A., Bettanini, C., Marchesi, M., Angrilli, F., "Self-balancing free flying 3D underactuated robot for zero-g object capture," 54th International Astronautical Congress of the International Astronautical Federation (IAF), the International Academy of Astronautics and the International Institute of Space Law, art. no. IAC-03-J.2.06, Vol. 2, pp. 2421-2431, 2003.
[60] Menon, C., Aboudan, A., Cocuzza, S., Bulgarelli, A., Bettanini, C., Marchesi, M., Angrilli, F., "Self-balancing free flying 3D underactuated robot for zero-g object capture," 54th International Astronautical Congress of the International Astronautical Federation (IAF), the International Academy of Astronautics and the International Institute of Space Law, art. no. IAC-03-J.2.06, Vol. 1, pp. 4325-4335, 2003.
[61] Umetani, Y., Yoshida, K., "Resolved Motion Rate Control of Space Manipulators with Generalized Jacobian Matrix," IEEE Transactions on Robotics and Automation, Vol. 5, No. 3, 1989, pp. 303–314.
[62] Lawson, C. L., Hanson, R. J., Solving Least Squares Problems, Society for Industrial and Applied Mathematics, Philadelphia, PA, 1987.
[63] Van Loan, C., "On the Method of Weighting for Equality-Constrained Least-Squares Problems," SIAM Journal of Numerical Analisys, Vol. 22, No. 5, 1985, pp. 851–864.
[64] Stewart, G. W., "On the Weighting Method for Least Squares Problems with Linear Equality Constraints," BIT Numerical Mathematics, Vol. 37, No. 4, 1997, pp. 961–967.